Photoinduced electron transfer in ruthenium(II) trisbipyridine complexes connected to a naphthalenebisimide *via* an oligo(phenyleneethynylene) spacer†

Frédérique Chaignon,[a] Fabien Buchet,[a] Errol Blart,[a] Magnus Falkenström,[b] Leif Hammarström*[b] and Fabrice Odobel*[a]

Received (in Montpellier, France) 26th June 2008, Accepted 31st October 2008
First published as an Advance Article on the web 16th December 2008
DOI: 10.1039/b810856k

The preparation and the characterization of three new dyads composed of a ruthenium trisbipyridine complex linked to a naphthalene bisimide electron acceptor *via* a phenyleneethynylene spacer of different length (one or two units) are reported. The dyads also differ by the anchoring position of the spacer on the bipyridine, which is appended either at the 4-position or the 5-position. Cyclic voltammetry and the UV-Vis absorption spectroscopy suggested that the spacer linked at the 5-position ensures a longer π-conjugation length but the electron transfer rates indicate a lower electronic coupling, than in 4-position. Photoinduced emission yields indicate a significant quenching of the MLCT excited-state of the ruthenium complex in these dyads. Except for the dyad linked in 5 position with one phenyleneethynylene unit, the transient absorption spectroscopy of all the other dyads evidences that the MLCT excited-state decays almost exclusively by electron transfer to form the charge-separated state Ru^{III}–NBI^{-}. This state could not be observed, presumably because the subsequent recombination to the ground state was much faster than its formation. In the dyad linked in 5 position with only one phenyleneethynylene unit, at room temperature, the ^{3}MLCT* state is in equilibrium with the ^{3}NBI* state, and it also decays *via* electron transfer. The notable feature of these dyads is first the occurrence of a relatively long-range electron transfer reaction *via* a bis(phenylethynylene) linking unit anchored at the 5 position. Secondly, we show within these series of compounds that subtle variations in the structure of the dyads (length of the spacer and anchoring position on bipy) have a strong impact on the rates and in the mechanism of decay of the ^{3}MLCT* state. The photophysical properties of the dyads can be explained in terms of energy proximity of different excited states and magnitude of the electronic coupling according to the anchoring position.

Introduction

The rational design of donor–bridge–acceptor (D–B–A) photomolecular system for photoinduced charge separation is of both fundamental and practical importance for solar energy conversion[1–3] and molecular electronics.[4–7] In D–B–A systems, the bridge plays a determining role because its electronic properties and its connectivity to A and to D control the rate of the electron transfer between D and A.[1,7–12] The search of bridging units that can act as molecular wires and promote electron transfer over very long distance with a substantial rate is of high interest, because they can be employed to produce long-lived charge separated-states and with high quantum yield.[13–19] The two latter features are the primary requirements that a system should fulfil in view of approaching the function of the photosynthetic reaction center. In this context, we have used oligophenylethynylene to connect porphyrin or phthalocyanine sensitizers and we showed that this type of bridge was particularly well-suited to assist photoinduced charge separation between these dyes.[20,21] The ruthenium tris(bipyridine) complex is a well-known sensitizer that has been extensively used as photoactive electron donor in dyads and triads molecular systems for light induced electron transfer.[22–24] In our continuing goal to design D–B–A systems performing bridge-mediated electron transfer, we were interested to use the ruthenium tris(bipyridine) complex as sensitizer, because its long-lived triplet MLCT excited-state and its strong oxidizing power after electron transfer (Ru^{III}) make it particularly appealing for this application. In a previous paper, we showed that the combination of a ruthenium tris(bipyridine) complex with a fullerene unit could lead to quantitative energy transfer upon excitation of the ruthenium complex, instead of the desired electron transfer.[25] This parasite reaction arises from the low lying level of the fullerene triplet excited-state. Naphthalene bisimide (NBI) has

[a] *CNRS, UMR 6230, Université de Nantes, CEISAM, Chimie Et Interdisciplinarité, Synthèse, Analyse, Modélisation, Faculté des Sciences et des Techniques, 2, rue de la Houssinière, BP 92208, 44322 NANTES Cedex 3, France. E-mail: Fabrice.Odobel@univ-nantes.fr; Fax: +33 2 51 12 54 02; Tel: +33 2 51 12 54 29*
[b] *Department of Photochemistry and Molecular Science, The Ångström Laboratories, Uppsala University, Box 523, SE-751 20 Uppsala, Sweden. E-mail: Leif.Hammarstrom@fotomol.uu.se; Fax: +46-18-471 6844; Tel: +46-18-471 3648*
† Dedicated to Prof. Jean-Pierre Sauvage on the occasion of his 65th birthday.

been used with success as an electron acceptor in association with porphyrin sensitizers[26–32] but with ruthenium complexes energy transfer sometimes occurs in conjunction with the charge separation reaction.[33–38] Moreover, in the ruthenium–fullerene dyads, we found unexpectedly that the energy transfer was essentially distance independent, giving the same rate constant for the dyads with one, two and three phenylene-ethylene groups in the bridge.[25] Various spectroscopic data showed that the nature of the ruthenium based excited state changed for the longest bridge, presumably from the usual metal-to-ligand charge transfer state to a state localized more on the bridge, with more π–π* character. We thus rationalized the similar energy transfer rate over distances from 1.1 to 2.3 nm by excitation energy hopping onto bridge states, which were thermally accessible also for the dyads with longer bridges.

In this study we have prepared new dyads to investigate if we could obtain a similarly distance-independent electron transfer *via* excitation energy hopping. To this end, the fullerene was replaced by naphthalene bisimide. Moreover we compare dyads with the bridge attached to either the 5-bpy or 4-bpy position. We finally varied the bridge length from one to two phenylethylene units, to obtain the dyads **D1p**, **D1m**, **D2p** and **D2m** (Chart 1). We show that the utilization of NBI instead of C_{60} can restore the desired electron transfer from the excited ruthenium tris(bipyridine) complex. In spite of the very similar intrinsic properties of the ruthenium complexes with different bridge attachment positions, the dyads show very different behavior. We show that it can be explained by the energy proximity of different excited states that makes the resulting properties of the dyads very sensitive to small variations in the structure.

Experimental

General

^{1}H and ^{13}C NMR spectra were recorded on a Bruker ARX 300 MHz or AMX 400 MHz Bruker spectrometer. Chemical shifts for ^{1}H NMR spectra are referenced relative to residual protons in the deuterated solvent ($CDCl_3$: δ = 7.26 ppm, MeOD: δ = 3.31 ppm). Mass spectra were recorded on a EI-MS HP 5989A spectrometer or on a JMS-700 (JEOL LTD, Akishima, Tokyo, Japan) double focusing mass spectrometer of reversed geometry equipped with electrospray ionization (ESI) source. Fast atom bombardment mass spectroscopy (FAB-MS) analyses were performed in *m*-nitrobenzyl alcohol matrix (MBA) on a ZAB-HF-FAB spectrometer. MALDI-TOF analyses were performed on an Applied Biosystems Voyager DE-STR spectrometer in positive linear mode at 20 kV acceleration voltage with α-cyano-4-hydroxycinnamic acid (CHCA) as matrix.

Thin-layer chromatography (TLC) was performed on aluminium sheets precoated with Merck 5735 Kieselgel 60F_{254}. Column chromatography was carried out either with Merck 5735 Kieselgel 60F (0.040–0.063 mm mesh) or with SDS neutral alumina (0.05–0.2 mm mesh). Air-sensitive reactions were carried out under argon in dry solvents and glassware.

Chemicals were purchased from Aldrich and used as received. Compounds 2,5-bis(dodecyloxy)-4-(2′-trimethylsilylethynyl)-iodobenzene **1**,[25] *N*-octyl-*N*′-(4′-iodophenyl)naphthalene-1,4,5,8-tetracarboxylic acid bisimide **4**,[39] ruthenium complexes **7**,[25] **9**,[39] **8**,[39] dyad **D1p**,[39] and reference complexes **R1p**,[39] **R2m**[25] and **R1m**[25] were prepared according to literature methods.

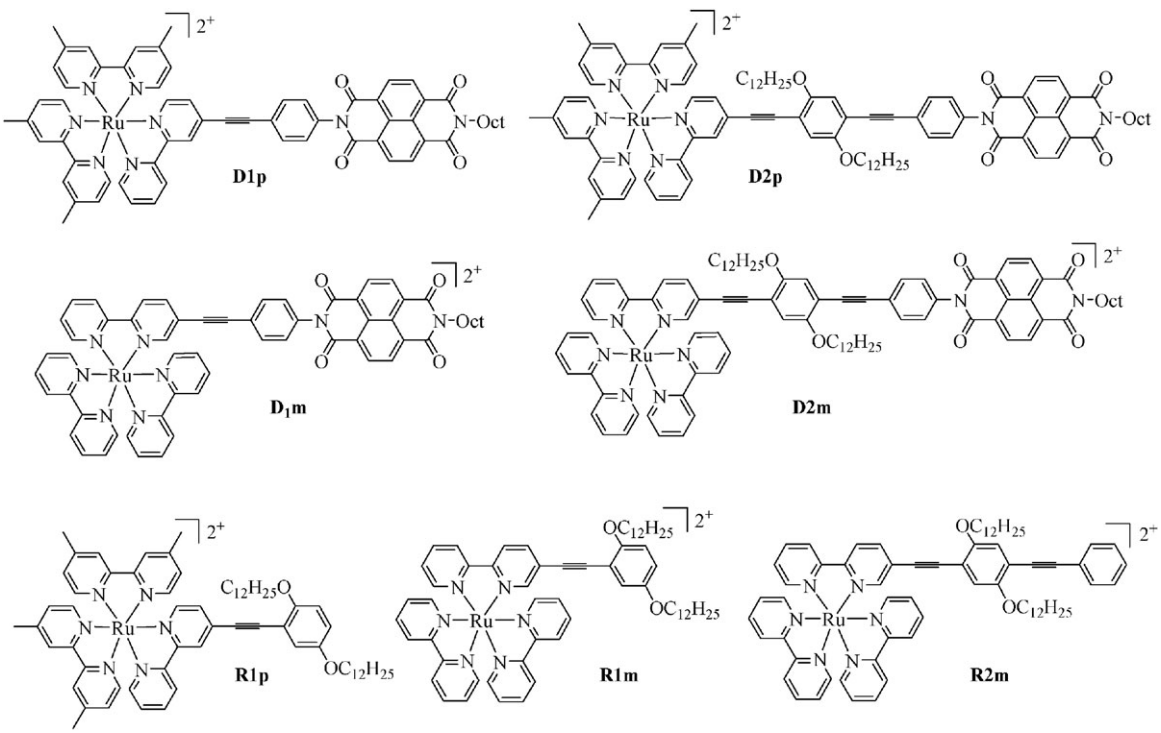

Chart 1 Structures of the molecules studied in this work.

The electrochemical measurements were performed with a potentiostat-galvanostat MacLab model ML160 controlled by resident software (Echem v1.5.2 for Windows) using a conventional single-compartment three-electrode cell. The working electrode was a 10 mm long Pt wire, the auxiliary was a Pt wire and the reference electrode was the saturated potassium chloride calomel electrode (SCE). The supported electrolyte was 0.1 M Bu_4NPF_6 in DMF and the solutions were purged with argon before the measurements. All potentials are quoted relative to SCE. In all the experiments the scan rate was 100 mV s^{-1} for cyclic voltammetry and 15 Hz for pulse voltammetry. The UV-Visible absorption spectra were recorded on a UV-2401PC Shimadzu spectrophotometer. Emission spectra were recorded on a SPEX Fluoromax fluorimeter and were corrected for the wavelength dependent response of the detector system (Hamamatsu R928).

Time-resolved emission and transient absorption spectra were recorded using an Applied Photophysics LKS60 laser-flash photolysis system. Excitation was obtained with 5 ns, 460 nm pulses (*ca.* 20 mJ $pulse^{-1}$) from a Q-switched YAG laser (Quantel Brilliant B) with an OPOTEK OPO. The detection system of the LKS60 employed a 150 W pulsed Xe-lamp for analyzing light at right angle configuration, a monochromator after the sample, a P928 PMT, and a digital oscilloscope (500 MHz, 2 Gs/s).

Syntheses

2,5-Bis(dodecyloxy)-4-(2′-trimethylsilylethynyl)triisopropylsilylacetylenylbenzene 2. A solution of compound **1** (0.4 g, 0.53 mmol) in dry triethylamine (2.7 mL) and tetrahydrofuran (0.9 mL) was introduced in a sealed tube and degassed by freeze–pump–thaw cycles. Then PPh_3 (21 mg, 0.080 mmol), $Cu(OAc)_2$ (5.3 mg, 0.026 mmol), $PdCl_2$ (9.5 mg, 0.053 mmol) and triisopropylsilylacetylene (0.3 mL, 1.33 mmol) were added. The reaction mixture was heated at 50 °C for 15 h. A saturated aqueous solution of NaCl was added and the solution was extracted with ethyl acetate. The organic layer was then washed with water, dried over $MgSO_4$, and rotary evaporated. The crude product was purified by flash chromatography (SiO_2, petroleum ether–diethyl ether: 100 : 0 to 99 : 1). **2** was obtained as a yellow oil (327 mg, 85%). ^{1}H NMR (300 MHz, $CDCl_3$): δ 6.89 (s, 1H), 6.88 (s, 1H), 3.94 (m, 4H), 1.77 (m, 4H), 1.27 (m, 20H), 1.15 (s, 21H), 0.89 (m, 6H), 0.27 (s, 9H). ^{13}C NMR (75 MHz, $CDCl_3$): δ 154.25, 153.99, 117.75, 116.73, 114.32, 113.89, 102.99, 101.31, 99.78, 96.43, 69.66, 69.28, 31.98, 29.69, 29.41, 26.21, 22.73, 18.74, 14.13, 11.43, 0.00. EI-MS$^+$: 169.25 (10%), 722.60 (14%).

2,5-Bis(dodecyloxy)-4-(2′-ethynyl)triisopropylsilylacetylenylbenzene 3. Compound **2** (175 mg, 0.24 mmol) was dissolved in dichloromethane (3.3 mL) and methanol (6.6 mL). Then potassium carbonate (0.33 g, 2.42 mmol) was added and the reaction mixture was stirred at room temperature for 3 h. Water was added and the solution was extracted with dichloromethane. The organic layer was washed with water, dried over $MgSO_4$ and rotary evaporated. **34** was obtained as a yellow oil (157 mg, quantitative). ^{1}H NMR (300 MHz, $CDCl_3$): δ 6.92 (s, 1H), 6.91 (s, 1H), 3.94 (m, 4H), 3.31 (s, 1H), 2.53 (s, 24H), 1.77 (m, 4H), 1.28 (m, 20H), 1.15 (s, 21H), 0.89 (m, 6H).

***N*-Octyl-*N*′-(2′,5′-bis(dodecyloxy)-4′-(2″-triisopropylsilylethynyl)-ethynylbenzene)naphthalene-1,4,5,8-tetracarboxylic acid bisimide 5.** A solution of compound **3** (157 mg, 0.24 mmol) and **4** (108 mg, 0.19 mmol) in dry triethylamine (6.5 mL) and tetrahydrofuran (4.5 mL) was introduced in a sealed tube and degassed by freeze–pump–thaw cycles. Then PPh_3 (7.3 mg, 0.028 mmol), $Cu(OAc)_2$ (1.9 mg, 0.009 mmol) and $PdCl_2$ (1.7 mg, 0.009 mmol) were added. The reaction mixture was heated at 70 °C for 15 h. The solvent was rotary evaporated and the crude product was purified by flash chromatography (SiO_2, petroleum ether–dichloromethane 15 : 85). **5** was obtained as a red solid (144 mg, 69%). ^{1}H NMR (300 MHz, $CDCl_3$): δ 8.80 (s, 4H), 7.71 (d, 2H, J = 8.4 Hz), 7.31 (d, 2H, J = 8.4 Hz), 6.96 (s, 1H), 6.94 (s, 1H), 4.21 (m, 2H), 3.99 (m, 4H), 1.80 (m, 6H), 1.27 (m, 46H), 1.15 (m, 21H), 0.85 (m, 9H).^{13}C NMR (75 MHz, $CDCl_3$): δ 162.71, 162.56, 154.24, 153.45, 134.16, 132.47, 131.27, 130.89, 128.58, 126.88, 126.68, 126.46, 124.57, 117.63, 116.32, 114.30, 113.58, 102.90, 96.60, 93.68, 87.31, 69.66, 69.26, 40.98, 31.86, 31.75, 29.61, 29.31, 29.15, 28.02, 27.04, 26.15, 26.01, 22.62, 18.68, 14.04, 11.35. HRES$^+$-MS: m/z: calc. for $C_{71}H_{99}N_2O_6$ 1103.7272; found 1103.7287 $[M + H]^+$.

***N*-Octyl-*N*′-(2′,5′-bis(dodecyloxy)-4′-(2″-ethynyl)ethynylbenzene)naphtalene-1,4,5,8-tetracarboxylic acid bisimide 6.** Compound **5** (144 mg, 0.13 mmol) was dissolved in tetrahydrofuran (11 mL) under argon. Then tetrabutylammonium fluoride (0.3 mL, 0.3 mmol) was added and the reaction mixture was stirred at 30 °C for 2 h. The solvent was rotary evaporated and water was added. The solution was extracted with dichloromethane and the organic layer was washed with water, dried over $MgSO_4$ and rotary evaporated. **6** was obtained as a red–brown solid (118 mg, 96%). ^{1}H NMR (300 MHz, $CDCl_3$): δ 8.79 (s, 4H), 7.71 (d, 2H, J = 8.4 Hz), 7.32 (d, 2H, J = 8.4 Hz), 6.96 (m, 2H), 4.21 (m, 2H), 3.99 (m, 4H), 3.35 (s, 1H), 1.80 (m, 6H), 1.27 (m, 46H), 0.85 (m, 9H).

Dyad D2m. A solution of complex **7** (92 mg, 0.098 mmol) and **6** (123 mg, 0.013 mmol) in dry triethylamine (0.96 mL) and dimethylformamide (6.4 mL) was introduced in a sealed tube and degassed by freeze–pump–thaw cycles. Then $Pd(dppf)Cl_2$ (15 mg, 0.020 mmol) and CuI (3.7 mg, 0.020 mmol) were added. The reaction mixture was heated at 45 °C for 15 h. Water was added and the solution was extracted with dichloromethane. The organic layer was then washed with water, dried over $MgSO_4$, and rotary evaporated. The crude product was purified by flash chromatography (SiO_2, dichloromethane–acetonitrile–KNO_3: 100 : 0 : 0 to 78 : 20 : 2). The dyad **D2m** was obtained as a red solid (60 mg, 33%). ^{1}H NMR (300 MHz, $CDCl_3$): δ 8.80 (s, 4H), 8.45 (m, 6H), 8.01 (m, 6H), 7.71 (m, 8H), 7.48 (m, 5H), 7.31 (d, 2H, J = 8.4 Hz), 6.98 (s, 1H), 6.97 (s, 1H), 4.21 (m, 2H), 3.98 (m, 4H), 1.80 (m, 6H), 1.27 (m, 46H), 0.85 (m, 9H). HRES$^+$-MS: m/z: calc. for $C_{92}H_{100}N_8O_6Ru$ 757.3405; found 757.3409 (M^{2+}).

Dyad D2p. A solution of complex **8** (80 mg, 0.080 mmol) and **6** (100 mg, 0.104 mmol) in dry triethylamine (0.8 mL) and dimethylformamide (5.2 mL) was introduced in a sealed tube and degassed by freeze–pump–thaw cycles. Then $Pd(dppf)Cl_2$

(12 mg, 0.016 mmol) and CuI (3 mg, 0.016 mmol) were added. The reaction mixture was heated at 75 °C for 15 h. Water was added and the solution was extracted with dichloromethane. The organic layer was then washed with water, dried over $MgSO_4$, and rotary evaporated. The crude product was purified by flash chromatography (SiO_2, dichloromethane–acetonitrile: 100 : 0 to 80 : 20). The dyad **D2p** was obtained as a red solid (69 mg, 46%).^{1}H NMR (300 MHz, $CDCl_3$): δ 8.80 (s, 4H), 8.31–8.21 (m, 7H), 7.97 (m, 1H), 7.78–7.70 (m, 4H), 7.52–7.46 (m, 7H), 7.33 (d, 2H, J = 8.4 Hz), 7.07 (s, 1H), 7.03 (s, 1H), 4.21 (m, 2H), 3.98 (m, 4H), 2.53 (m, 12H), 1.80 (m, 6H), 1.27 (m, 46H), 0.85 (m, 9H). HRES$^+$-MS: m/z: calc. for $C_{96}H_{108}N_8O_6Ru$ 785.3712; found 785.3698 (M^{2+}).

Dyad D1m. NBI derivative **9** (57 mg, 0.11 mmol), ruthenium complex **7** (85 mg, 0.09 mmol), $Pd(dppf)Cl_2$ (14.5 mg, 0.02 mmol) and CuI (3.7 mg, 0.02 mmol) were introduced in a sealed tube, then dry triethylamine (0.5 ml) and anhydrous dimethylformamide (5 ml) were added and the resulting mixture was degassed by three freeze–pump–thaw cycles. The solution was heated at 80 °C for 17 h. The reaction mixture was then concentrated on a rotary evaporator to remove most of the solvent and the residue was diluted with dichloromethane. The organic layer was washed with an aqueous solution of NH_4Cl, then water and finally with brine and dried over $MgSO_4$ and concentrated *in vacuo* to dryness. The crude red solid was purified by flash column chromatography (SiO_2, acetone–water–saturated aqueous KNO_3 solution 9 : 1 : 0.002 to 9 : 1 : 0.004) to give the desired compound as a dark red solid (66 mg, 55%). ^{1}H NMR (300 MHz, CD_3CN): δ 8.70 (dd, 4H, J = 12.3, 7.7 Hz), 8.48–8.54 (m, 6H), 8.19 (dd, 1H, J = 8.4, 1.8 Hz), 8.03–8.12 (m, 5H), 7.90 (br. d, 1H, J = 1.3 Hz), 7.85 (br. d, 1H, J = 5.7 Hz), 7.70–7.77 (m, 4H), 7.67 (d, 2H, J = 8.55 Hz), 7.44 (d, 2H, J = 8.55 Hz), 7.37–7.45 (m, 4H), 4.13 (dd, 2H, J = 9.0, 7.5 Hz), 1.68–1.77 (m, 2H), 1.27–1.42 (m, 10H), 0.88 (t, 3H, J = 6.8 Hz). ^{13}C NMR (75 MHz, CD_3CN): δ 164.02, 163.78, 157.96, 157.91, 157.88, 157.84, 157.10, 154.28, 152.95, 152.76, 152.73, 152.70, 152.51, 140.73, 138.87, 138.78, 137.88, 133.43, 131.58, 131.34, 130.47, 128.62, 128.59, 128.52, 128.10, 127.82, 127.74, 127.60, 125.70, 125.35, 125.23, 124.87, 124.52, 122.73, 99.35, 85.75, 41.47, 32.47, 29.91, 29.86, 28.54, 27.75, 23.30, 14.32. MALDI-MS: m/z: calc. for $C_{60}H_{48}N_8O_4RuPF_6^+$ 1192.2; found 1191.9 $[M - PF_6^-]^+$.

Results and discussion

Synthesis of the compounds

The key step of the synthesis of the new dyads **D1m**, **D2m** and **D2p** is the Sonogashira cross-coupling reaction between the synthon **6** or **9**[39]and the bromobipyridine ruthenium complex **7**[25]and **8**[25,40] (Scheme 1). The synthesis of the key intermediate **6** is depicted in Scheme 2 and it starts with the known bisalkoxy *para*-(trimethylsilylethynyl)iodobenzene **1**[25] which was initially coupled with triisopropylsilylacetylene using the classical conditions of Sonogashira reaction to afford **2** with 85% yield. The trimethylsilyl group was then cleaved with potassium carbonate in a quantitative yield and the resulting compound **3** was connected to the iodonaphthalene bisimide **4**[39] to give **5** in 69% isolated yield (Scheme 2). The last step consists of a final Sonogashira cross-coupling reaction, directly made on the complex (**7** or **8**) with the NBI derivative **6** or **9** (Scheme 1). The diphenylphosphinoferrocene (dppf) was chosen as ligand of palladium in the catalytic system of this last coupling because it proved to be particularly well-suited in previously reported cross-coupling reactions carried out on a ruthenium complex.[25,41] The dyads **D2m**, **D2p** and **D1m** were thus respectively obtained in 33, 46 and 55% yield after purification on column chromatography.

Electronic absorption spectra

The absorption spectra of the dyads **D1p**, **D1m**, **D2p**, **D2m** are shown in Fig. 1 and the spectroscopic data are collected in Table 1. The most intense absorption in the UV, at around 290 nm, is assigned to a π–π* transition localized on the bipyridine ligands. The two sharp absorptions at 360 and 380 nm are attributed to the NBI unit and are almost not affected by comparison with the parent compound **4**.[25,42] This is consistent with the presence of nodes of the frontier molecular orbitals on the nitrogens of the imide groups, which lead to weak electronic communication with any substituents attached on these positions.[39,43] Accordingly, the absorption bands of the ruthenium complex and of those of the phenylethynylene spacer are not affected by the presence of the NBI, as confirmed by the similar maximum absorption wavelengths of these transitions in the dyads compared to those in the parent reference compounds (Table 1). The π–π* transition of the oligophenylethynylene spacer occurs at 390 nm in dyads **D2m–D2p** and is naturally blue-shifted in dyad **D1p** and **D1m** containing the shorter linker. The broad absorption band in the visible region is attributed to the well-known spin-allowed metal-to-ligand charge transfer transition (MLCT). Interestingly, this absorption band is less intense and blue-shifted in the dyads **D2m** and **D1m** in which the spacer is attached in the 5 position of the bipyridine compared to the other dyads linked on the 4 position. The same effect has been observed in other tris-bipyridine ruthenium complexes functionalized either on the 4 position or on the 5 position of the bipyridine.[44–48]

Electrochemical study

The dyads were studied by cyclic voltammetry and differential pulse voltammetry in DMF and the half-wave potentials are collected in Table 2. The first oxidation reaction is a ruthenium-centred process which involves the $\pi(t_{2g})$ metal orbital. In dyads **D1p** and **D2p**, the potential is cathodically shifted by 100 mV compared to that in dyad **D2m** and **D1m**, and to the unsubstituted $[Ru(bpy)_3]^{2+}$ (Table 2). This is attributed mainly to the consequence of electron donating methyl substituents, borne on the ancillary bipyridine of the former complexes, which stabilize the Ru(III).[49] The two first reductions, taking place at about −0.45 and −1 V, respectively, correspond to the consecutive one-electron reductions of the NBI unit,[42] while the third reduction, at around −1.2 V, is attributed to the reduction of the bipyridine ligand that is connected to the spacer. The third reduction is easier in the dyads **D1p**, **D1m**, **D2p**, **D2m** with respect to the unsubstituted

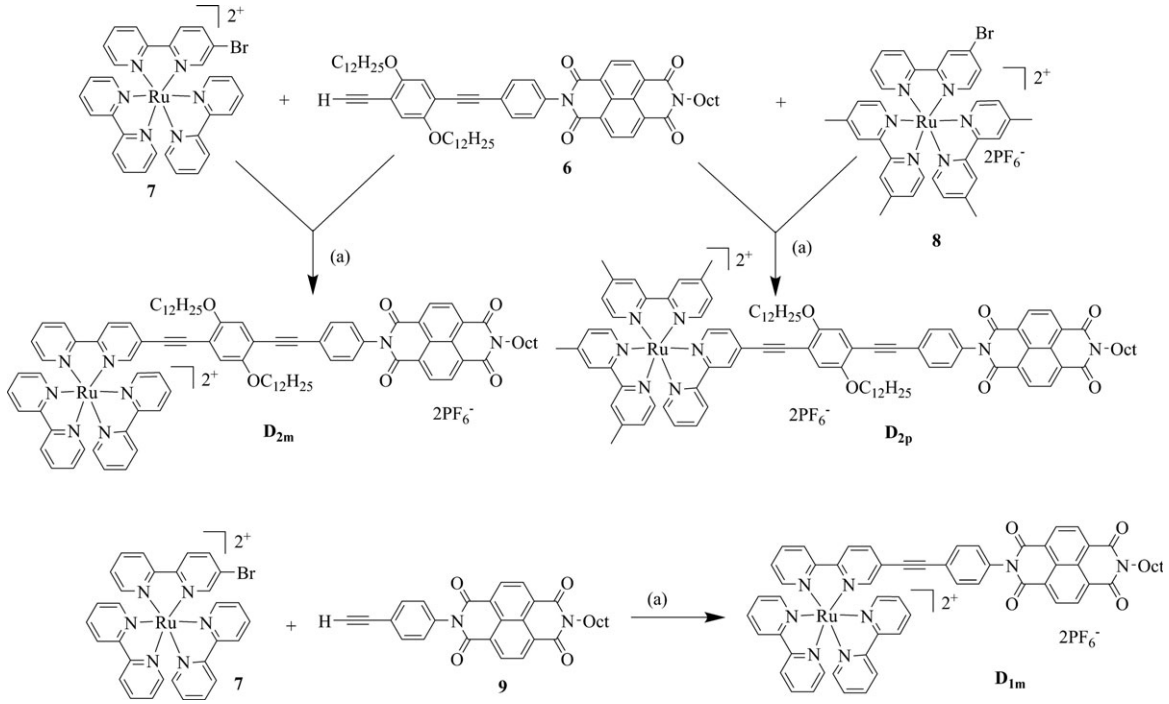

Scheme 1 *Reagents and conditions:* (a) $Pd(dppf)Cl_2$, CuI, Et_3N, DMF (33% for **D2m**, 46% for **D2p** and 55% for **D1m**).

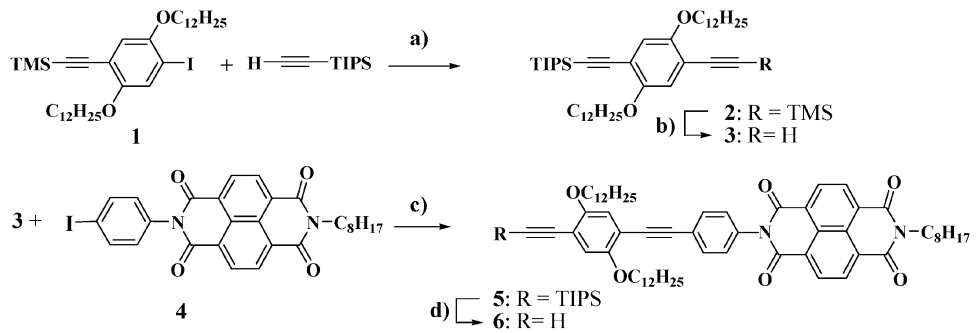

Scheme 2 *Reagents and conditions:* (a) $Pd(PPh_3)_2Cl_2$, $Cu(OAc)_2$, Et_3N, THF, 50 °C (85%); (b) K_2CO_3, CH_2Cl_2–CH_3OH, RT (100%); (c) $Pd(PPh_3)_2Cl_2$, $Cu(OAc)_2$, Et_3N, THF, 70 °C (69%); (d) Bu_4NF, THF, RT (100%).

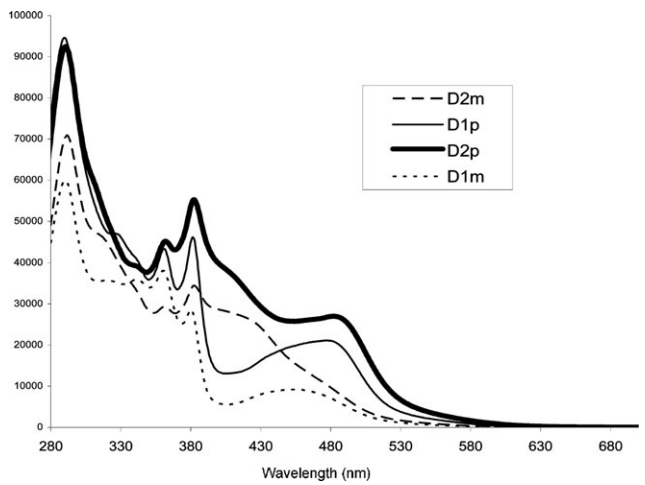

Fig. 1 Absorption spectrum of the dyads **D1p**, **D1m**, **D2p** and **D2m** recorded in DMF.

$[Ru(bpy)_3]^{2+}$; this indicates a stabilization of the π* orbital upon the attachment of the spacer. It results from an increased π-conjugation length between the bipyridine and the oligo-ethynylenephenylene spacer as already observed when a π-conjugated spacer is linked to a polypyridine ruthenium complex.[25,39,50–54] Interestingly, the stabilization of the LUMO orbital of the bipyridine is less marked when the spacer is connected on the 4 position (**D1p** or **D2p**) compared to the 5 position of bipyridine (**D1m** or **D2m**). This suggests a longer π-conjugation length when the bipyridine is substituted on the 5 position, probably due to a higher spin density of the LUMO orbital at this position and the larger number of mesomer structures between the pyridines and the oligo(phenyleneethynylene) spacer.[55,56]

Steady-state and time-resolved emission

The luminescence properties of the dyads **D1p**, **D1m**, **D2p**, **D2m** were studied by steady-state and time-resolved spectroscopy and were compared to the reference compounds

Table 1 UV-Vis and emission data of the complexes

Complex	λ_{max}^{Abs}/nm (ε/M^{-1} cm^{-1})[a]	λ_{em}/nm (RT)[a]	λ_{em}/nm (77 K)[b]	E_{00}/eV (^{3}MLCT)[c]
R1p	477 (14800), 372 (14200), 348 (14100), 291 (62000)	655	626	1.98
R2m	407 (35400), 310 (52600), 291 (75400)	671	617	2.01
NBI **4**	360, 380	368	608	2.04
D1p	477 (21100), 381 (45600), 361 (42800), 325 (46350), 289 (94000)	674	636	1.94
D2m	410 (27800), 383 (34000), 361 (29400), 313 (47100), 292 (71000)	668	618	2.01
D2p	482 (27000), 382 (55200), 362 (45100), 291 (92500)	676	636	1.94
D1m	456 (9200) 380 (29100), 361 (38600), 342 (36600), 290 (60700)	670	618	2.01

[a] Recorded in DMF. [b] Recorded in ethanol–methanol glass. [c] Calculated from the emission maximum at 77 K (E_{00} = 1240/$\lambda_{em(77\ K)}$).

Table 2 Redox potentials of the dyads recorded in DMF with Bu_4NPF_6 (0.1 M) as supporting salt. The potentials are quoted *vs.* saturated calomel electrode (SCE)

	$E_{Ox}(Ru^{III}/Ru^{II})$/V	E_{Red1}(NBI/NBI^-)/V	E_{Red2}(NBI^-/NBI^{2-})/V	E_{Red3}(bpy/bpy^-)/V
$[Ru(bpy)_3]^{2+}$	1.30			−1.24
D1p	1.21	−0.46	−0.95	−1.18
D2m	1.32	−0.47	−0.97	−1.04
D2p	1.21	−0.47	−0.95	−1.18
D1m	1.33	−0.47	−0.94	−1.11

(**R1p**, **R2m** and **R1m**) to determine the quenching efficiency of the MLCT excited-state by the nearby NBI electron acceptor.‡ Table 3 collects the emission lifetimes, the quenching percentage and the quenching rate of the MLCT emission. The broad emission band in the above compounds is attributed to the phosphorescence of the triplet MLCT excited-state of the ruthenium complex. At 77 K a vibronic structure typical for ^{3}MLCT emission of Ru(II)polypyridyl complexes is observed (see ref. 25 for spectra of **R2m** and **R1m**). In previous studies,[25] our spectroscopic data suggested that with a tris(phenylethylene) spacer in the 5-bpy position of the ruthenium complex, the lowest excited-state of the system can be assigned to a triplet π–π* of the spacer.[25,51,57–59] In contrast, for the mono- and bis(phenylethylene) complexes the ^{3}MLCT state was the lowest excited state. Referring to previous work, the lowest excited state is ^{3}MLCT in all of the present dyads.[25]

The energy of the MLCT excited state was determined from the emission spectrum recorded in ethanol glass at 77 K and it shows that in the dyads **D1p** and **D2p** this level is lower lying than that in **D2m** and **D1m** (Table 1). This can be explained by the inductive effect of the methyl substituents on the bipyridines of **D1p** and **D2p** that destabilize the π(t_{2g}) HOMO orbitals and decrease the energy gap with the π* LUMO orbital on the bipyridine, whereas the longer π-conjugation of the bpy with the bridge in **D2m** and **D1m** stabilizes the LUMO orbitals, but to an overall lower extent.

The emission lifetime measurements, made in degassed acetonitrile solution, indicate a significant shortening of the MLCT emission in the dyads **D1p**, **D1m**, **D2p** and **D2m** compared to those in the reference complexes (Table 3). The quenching rate of the ruthenium by the NBI decreases in the following order **D1p** > **D2m** > **D1m** > **D2p**.

In dyads **D1p**, **D2p** and **D2m**, the transient absorption shows only the features of the initial ^{3}MLCT state, which decays with the same time constant as the emission decay. Therefore, in the dyads **D1p**, **D2p** and **D2m** the most plausible interpretation of the results is an electron transfer process leading to Ru^{III}–NBI^-, which recombines with a faster rate than that of its formation. This is in analogy to our previous study of **D1p** and a related dyad, but where the electron transfer products were sufficiently long-lived to be detected. In the dyad **D1m** the decay of the emission and transient absorption signals are instead biexponential. A global fit to the transients at 360–700 nm gave time constants of 120 and 420 ns. The initial spectrum is identical to that for the **R1p** reference, while the spectrum that emerges after the faster phase can be assigned to a mix of the original ^{3}MLCT state and the ^{3}NBI state (Fig. 2). These two species decay simultaneously with a 420 ns time constant. The transient traces around 480 nm show a clear rise-and-decay behavior as the ^{3}NBI is formed and then disappears.[60] The results are consistent with electron transfer from the ^{3}MLCT state to the NBI unit, in parallel to excited state equilibration by triplet energy transfer between the ^{3}MCLT and ^{3}NBI states. After equilibration the excited states are depopulated by further electron transfer *via* the ^{3}MLCT state (Scheme 3). From a kinetic analysis in the

Table 3 Emission lifetimes (τ_{em}) and electron transfer rate constants (k_{ET}) in degassed acetonitrile at room temperature

	τ_{em}/ns	% quenching[a]	k_{ET}[b]/s^{-1}	ΔG^0_{ET}[c]/eV
R1p	1500	—	—	—
R2m	1400	—	—	—
R1m	1200	—	—	—
D1p	63	96	1.5×10^7	−0.27
D2m	200	86	4.3×10^6	−0.22
D2p	900	40	4.4×10^5	−0.26
D1m	120, 420	73	3×10^6	−0.21

[a] Calculated as 100(τ_0 − τ_{em})/τ_0, where τ_0 is τ_{em} of the corresponding reference **R1p** or **R2m**. [b] Calculated as k_q = 1/τ_{em} − 1/τ_0. [c] Calculated as ΔG^0_{ET} = $e(E^0(Ru^{III}/Ru^{II}) - E^0(NBI/NBI^-)) - E_{00}(^3MLCT)$ taken from Tables 1 and 2. Work terms and differences between redox potentials in DMF (ε = 38) and CH_3CN (ε = 37) were neglected.

‡ From comparison with previous studies, the longer spacer in **D2p** than **R1p** would lead to an most 20% underestimation of the unquenched lifetime with the longer spacer and consequently at most a 10% underestimation of the electron transfer rate constant in **D2p**.[25]

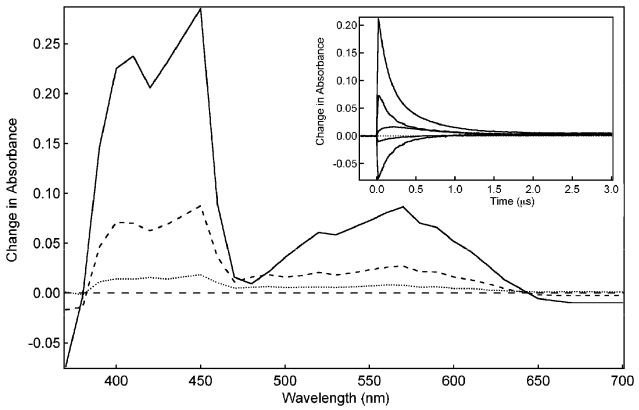

Fig. 2 Transient absorption spectra of **D1m** after excitation at 440 nm, after 30 ns (solid), 300 ns (dashed) and 1000 ns (dotted). Inset: transient absorption traces of the same experiments, at (from top to bottom) 450, 580, 480, 670 and 370 nm.

Appendix, the individual rate constants can be calculated to give $k_{ET} = 5 \times 10^6\ s^{-1}$, while the charge recombination (k_{CR}) is again much faster so that no charge separated state can be observed, just as for the other dyads.

The ratio of the energy transfer rate constants k_{EnT} and k_{-EnT} in Scheme 3 is close to unity, which means that the ^{3}MLCT and ^{3}NBI states in **D1m** lie at very similar energy. For the dyads **D1p** and **D2p**, linked in the 4-bpy position, the ^{3}MLCT states are lower in energy. This can explain why energy transfer to form ^{3}NBI was not observed in **D1p** and **D2p**. Also for **D2m**, which is linked in the 5-bpy position, the ^{3}MLCT should be slightly lower than in **D1m**, due to the longer π-delocalization on the bridge (as evidenced by the lower reduction potential of bipy in **D2m** than in **D1m**, Table 2) and we did not obtain clear evidence for energy transfer in **D2m**. A minor transient component (5%) with a longer, *ca.* 1000 ns lifetime, was indeed observed, but the signal was small and the lifetime was similar to that for the reference, so we could not determine if there was any ^{3}NBI contribution or if it can be attributed to a minor, unquenched ^{3}MCLT population. In any case, the small magnitude means that the possible effect on the calculated rate constant for electron transfer in **D2m** is small, giving an error of at most 10%.

The normal distance dependence of the electron transfer rate in **D1p** and **D2p** is an interesting contrast to the results of the other two dyads. If the putative, more bridge-localized state responsible for the distance-independent electron transfer in **D2m** and **D1m** were just another ^{3}MLCT state, one could

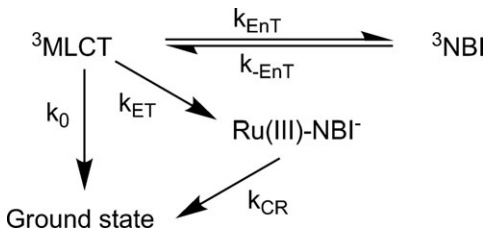

Scheme 3 Reaction scheme for **D1m** after MLCT excitation of the ruthenium complex.

expect that its energy would also be lower for **D1p** and **D2p**, and that therefore it would be just as thermally accessible. Instead, if it is more a bridge-localized π–π* state, its energy should be almost independent of anchoring position. Thus, it would be somewhat higher lying relative to the energy of ^{3}MLCT state in **D1p** and **D2p** and as a result they should not be as easily populated as in **D2m** and **D1m**. Indeed, the 30× difference in rate for the former, with a distance difference of 8 Å, is consistent with a distance decay factor "β" of 0.4 $Å^{-1}$, which is normal for a super-exchange mediated electron transfer with this chromophore-conjugated bridge combination.[20,61]

Note added in proof: Harriman and co-workers[62] have pointed out the importance of bending flexibility of the phenylethenyl bridges. They presented molecular modeling simulations suggesting that the $Ru(bpy)_3$ and C_{60} moieties in a Ru–C_{60} dyad bridged by one phenylethenyl unit frequently come into van der Waals contact, and suggested that electron and energy transfer processes may occur through close through-space contact and not through the bridge. While this may be correct for the shorter bridge, a close contact is not possible in the dyads with two or three bridge units, however. The flexibility of the bridge can therefore not explain the distance independent reaction rates in the series of 5-bpy bridged Ru-C_{60} presented earlier[25] or in the Ru–NBI dyads presented here.

Conclusion

The preparation and characterizations of three new dyads composed of a ruthenium trisbipyridine complex and a naphthalene bisimide electron acceptor are described. In the three dyads **D1p**, **D2m** and **D2p** the ruthenium trisbipyridine sensitizer decays almost exclusively by an electron transfer instead of an energy transfer process as observed in our previous systems in which the NBI was replaced by the fullerene.[25] As a result, these new dyads constitute a significant improvement over the previous ones. The present results show the following effects of the structural variations of the dyads discussed in the introduction. First, the replacement of C_{60} with NBI as acceptor makes energy transfer less probable and opens for charge separation reactions. Second, the alternation between 4- and 5-bpy substitutions shows different effects that can be related both to the intrinsic difference in bridge-chromophore coupling and to the proximity of the ^{3}MLCT, ^{3}NBI and bridge excited states: on the one hand, the electronic coupling is stronger *via* the 4-bpy than *via* the 5-bpy position. This is shown by comparison of the two dyads with the short links, where **D1p** shows a faster electron transfer than **D1m**. On the other hand, the dyads with the longer bridges show the opposite behavior: electron transfer is much faster in the 5-bpy substituted dyad **D2m**. This leads to the interesting observation that while the 4-bpy linked dyads show a 30-fold slower electron transfer with addition of another phenyleneethylene group, electron transfer is equally fast in **D2m** and **D1m**, in spite of the 8 Å difference in distance. The near-independence on electron transfer distance in the 5-bpy linked dyads parallels our previous results on triplet energy transfer in the analogous 5-bpy linked Ru–C_{60} dyads.[25] We concluded in that

paper, based on various spectroscopic data, that the lowest excited-state of the Ru-bridge system was gradually shifted more onto the bridge as the latter became longer, which could explain the observed near-independence on bridge length on the energy transfer rate. In the present study we seem to observe an analogous effect for electron transfer. In summary, we showed within these series of dyads that subtle structural changes result in significant modifications of the rate and of the mechanism of electron transfer from the ruthenium complex to NBI. More precisely, the energy level of the ^{3}MLCT* and/or the electronic coupling, which can be tuned by changing the length of the spacer, its anchoring position or the presence of the methyl groups on the bpy, govern the feasibility of the energy transfer to NBI. This information can be useful for the future design of photomolecular systems for photoinduced charge separation with ruthenium trisbipyridine sensitizer. Interestingly, the dyad **D2m** containing the bis(phenylethynylene) spacer appended in the 5-position of the bipyridine represents a potentially useful molecular basis to build multicomponent systems for long-range photoinduced charge separation since long range electron transfer occurs with a high quantum yield at room temperature in acetonitrile (86%).

Appendix

Derivation of the rate constants for D1m according to Scheme 3

The reaction scheme has the following solution:[63,64]

$$\theta_1 + \theta_2 = k_0 + k_{ET} + k_{EnT} + k_{-EnT} \quad \text{(A1)}$$

$$-(k_0 + k_{ET}) - (1 + N_{MLCT}/N_{NBI})k_{EnT} + (1 + N_{NBI}/N_{MLCT})k_{-EnT} \quad \text{(A2)}$$

where θ_1 and θ_2 are the experimentally observed rate constants 8.3×10^6 and 2.4×10^6 s^{-1}, respectively, and the ratios are the relative populations of the ^{3}MLCT and ^{3}NBI states. We determined the difference in extinction coefficient for the ^{3}MLCT state at 570 nm as $\Delta\varepsilon = 8 \times 10^3$ M^{-1} cm^{-1} by comparison with the 450 nm bleach of $[Ru(bpy)_3]^{2+}$ ($\Delta\varepsilon = 1.0 \times 10^4$ M^{-1} cm^{-1})[65] under the same conditions in flash photolysis experiments. Also for ^{3}NBI at 480 nm $\Delta\varepsilon = 8 \times 10^3$ M^{-1} cm^{-1}.[60] With these values we determined that the relative population of these states after establishment of quasi-equilibrium is about unity (dashed spectrum in Fig. 2). In the scheme the only quenching of ^{3}MLCT emission is due to the competition between k_{ET} and k_0. With $k_0 = 9 \times 10^5$ s^{-1} as in the reference **R1m**, and from the relative emission yield $\Phi_{rel} = k_0/(k_0 + k_{ET}) = 0.27$, we obtain $k_{ET} = 3 \times 10^6$ s^{-1}. From eqn (A1) and (A2), and the condition $k_{EnT} = k_{-EnT}$, we then obtain a value of 3×10^6 s^{-1} for the latter two rate constants.

The time-resolved emission data show that about 2/3 of the emitted photons lie in the 420 ns component (from the integrated areas under the emission traces), which means that about 2/3 of the initially formed excited state remains after the 120 ns phase. With the approximately equal concentrations of ^{3}MLCT and ^{3}NBI states at quasi-equilibrium one would expect to see a ^{3}MLCT transient signal, just when equilibrium is obtained, that is about 1/3 of the initial signal. This is indeed the case (Fig. 2). This good agreement suggests that electron transfer from the ^{3}NBI state is negligible and gives *a posteriori* support for Scheme 3. The accuracy of the value determined for k_{ET} is obviously less than for a direct observation in the absence of complicating parallel reactions. Nevertheless, the corresponding time constant of *ca.* 300 ns, as reported in Table 3, is clearly not shorter than for **D2m** with the longer bridge.

Acknowledgements

The French Research Ministry is gratefully acknowledged for the financial support of these researches through the programs "ACI Jeune Chercheur" and the ANR blanc "PhotoCumElec" and the European Community for COST D35 program. L. H. acknowledges support from the K&A Wallenberg Foundation, the Swedish Energy Agency and the Swedish Foundation for Strategic Research and thanks Dr Amanda Smeigh for fitting and plotting the transient absorption data.

References

1 V. Balzani and F. Scandola, *Supramolecular Photochemistry*, Ellis Horwood, Chichester, UK, 1991.
2 M. A. Fox and M. T. Dulay, *Chem. Rev.*, 1993, **93**, 341–357.
3 J. H. Alstrum-Acevedo, M. K. Brennaman and T. J. Meyer, *Inorg. Chem.*, 2005, **44**, 6802–6827.
4 J. Park, N. Pasupathy Abhay, I. Goldsmith Jonas, C. Chang, Y. Yaish, R. Petta Jason, M. Rinkoski, P. Sethna James, D. Abruna Hector, L. McEuen Paul and C. Ralph Daniel, *Nature*, 2002, **417**, 722–725.
5 C. Joachim, J. K. Gimzewski and A. Aviram, *Nature*, 2000, **408**, 541–548.
6 J. M. Tour, *Acc. Chem. Res.*, 2000, **33**, 791–804.
7 *Molecular Electronics*, ed. J. Jortner and M. Ratner, Blackwell Science, London, 1997.
8 M. Bixon and J. Jortner, *Adv. Chem. Phys.*, 1999, **106**, 35–202.
9 D. M. Adams, L. Brus, C. E. D. Chidsey, S. Creager, C. Creutz, C. R. Kagan, P. V. Kamat, M. Lieberman, S. Lindsay, R. A. Marcus, R. M. Metzger, M. E. Michel-Beyerle, J. R. Miller, M. D. Newton, D. R. Rolison, O. Sankey, K. S. Schanze, J. Yardley and X. Zhu, *J. Phys. Chem. B*, 2003, **107**, 6668–6697.
10 A. C. Benniston and A. Harriman, *Chem. Soc. Rev.*, 2006, **35**, 169–179.
11 B. P. Paulson, J. R. Miller, W.-X. Gan and G. Closs, *J. Am. Chem. Soc.*, 2005, **127**, 4860–4868.
12 M. P. Eng and B. Albinsson, *Angew. Chem., Int. Ed.*, 2006, **45**, 5626–5629.
13 W. B. Davis, W. A. Svec, M. A. Ratner and M. R. Wasielewski, *Nature*, 1998, **396**, 60–63.
14 R. F. Kelley, M. J. Tauber and M. R. Wasielewski, *Angew. Chem., Int. Ed.*, 2006, **45**, 7979–7982.
15 R. F. Kelley, M. J. Tauber, T. M. Wilson and M. R. Wasielewski, *Chem. Commun.*, 2007, 4407–4409.
16 C. Atienza-Castellanos, M. Wielopolski, D. M. Guldi, C. van der Pol, M. R. Bryce, S. Filippone and N. Martin, *Chem. Commun.*, 2007, 5164–5166.
17 G. De la Torre, F. Giacalone, J. L. Segura, N. Martin and D. M. Guldi, *Chem.–Eur. J.*, 2005, **11**, 1267–1280.
18 S. A. Vail, P. J. Krawczuk, D. M. Guldi, A. Palkar, L. Echegoyen, J. P. C. Tome, M. A. Fazio and D. I. Schuster, *Chem.–Eur. J.*, 2005, **11**, 3375–3388.
19 F. Giacalone, J. L. Segura, N. Martin, J. Ramey and D. M. Guldi, *Chem.–Eur. J.*, 2005, **11**, 4819–4834.
20 J. Fortage, E. Goeransson, E. Blart, H.-C. Becker, L. Hammarström and F. Odobel, *Chem. Commun.*, 2007, 4629–4631.
21 J. Fortage, J. Boixel, E. Blart, L. Hammarström, H.-C. Becker and F. Odobel, *Chem.–Eur. J.*, 2008, **14**, 3467–3480.

22 J. P. Sauvage, J. P. Collin, J. C. Chambron, S. Guillerez, C. Coudret, V. Balzani, F. Barigelletti, L. De Cola and L. Flamigni, *Chem. Rev.*, 1994, **94**, 993–1019.
23 V. Balzani, A. Juris, M. Venturi, S. Campagna and S. Serroni, *Chem. Rev.*, 1996, **96**, 759–834.
24 M. H. V. Huynh, D. M. Dattelbaum and T. J. Meyer, *Coord. Chem. Rev.*, 2005, **249**, 457–483.
25 F. Chaignon, J. Torroba, E. Blart, M. Borgström, L. Hammarström and F. Odobel, *New J. Chem.*, 2005, **29**, 1272–1284.
26 R. F. Kelley, M. J. Tauber and M. R. Wasielewski, *J. Am. Chem. Soc.*, 2006, **128**, 4779–4791.
27 I.-W. Hwang, M. Park, T. K. Ahn, Z. S. Yoon, D. M. Ko, D. Kim, F. Ito, Y. Ishibashi, S. R. Khan, Y. Nagasawa, H. Miyasaka, C. Ikeda, R. Takahashi, K. Ogawa, A. Satake and Y. Kobuke, *Chem.–Eur. J.*, 2005, **11**, 3753–3761.
28 K. Okamoto, Y. Mori, H. Yamada, H. Imahori and S. Fukuzumi, *Chem.–Eur. J.*, 2004, **10**, 474–483.
29 N. Yoshida, T. Ishizuka, K. Yofu, M. Murakami, H. Miyasaka, T. Okada, Y. Nagata, A. Itaya, H. S. Cho, D. Kim and A. Osuka, *Chem.–Eur. J.*, 2003, **9**, 2854–2866.
30 H. Imahori, H. Yamada, D. M. Guldi, Y. Endo, A. Shimomura, S. Kundu, K. Yamada, T. Okada, Y. Sakata and S. Fukuzumi, *Angew. Chem., Int. Ed.*, 2002, **41**, 2344–2347.
31 C. A. Hunter and R. K. Hyde, *Angew. Chem., Int. Ed. Engl.*, 1996, **35**, 1936–1939.
32 A. Osuka, R. P. Zhang, K. Maruyama, T. Ohno and K. Nozaki, *Chem. Lett.*, 1993, 1727–1730.
33 F. Chaignon, E. Blart, M. Borgström, L. Hammarström and F. Odobel, *Actual. Chim.*, 2006, **297**, 23–27.
34 M. Borgström, N. Shaikh, O. Johansson, M. F. Anderlund, S. Styring, B. Aakermark, A. Magnuson and L. Hammarström, *J. Am. Chem. Soc.*, 2005, **127**, 17504–17515.
35 O. Johansson, H. Wolpher, M. Borgström, L. Hammarström, J. Bergquist, L. Sun and B. Kermark, *Chem. Commun.*, 2004, 194–195.
36 O. Johansson, M. Borgström, R. Lomoth, M. Palmblad, J. Bergquist, L. Hammarström, L. Sun and B. Kermark, *Inorg. Chem.*, 2003, **42**, 2908–2918.
37 D. W. Dixon, N. B. Thornton, V. Steullet and T. Netzel, *Inorg. Chem.*, 1999, **38**, 5526–5534.
38 M. D. Hossain, M.-a. Haga, H. Monjushiro, B. Gholamkhass, K. Nozaki and T. Ohno, *Chem. Lett.*, 1997, 573–574.
39 F. Chaignon, M. Falkenström, S. Karlsson, E. Blart, F. Odobel and L. Hammarström, *Chem. Commun.*, 2007, 64–66.
40 C. Goze, D. V. Kozlov, F. N. Castellano, J. Suffert and R. Ziessel, *Tetrahedron Lett.*, 2003, **44**, 8713–8716.
41 D. J. Hurley and Y. Tor, *J. Am. Chem. Soc.*, 2002, **124**, 3749–3762.
42 D. Gosztola, M. P. Niemczyk, W. Svec, A. S. Lukas and M. R. Wasielewski, *J. Phys. Chem. A*, 2000, **104**, 6545–6551.
43 F. Würthner, S. Ahmed, C. Thalacker and T. Debaerdemaeker, *Chem.–Eur. J.*, 2002, **8**, 4742–4750.
44 R. Argazzi, C. A. Bignozzi, T. A. Heimer, F. N. Castellano and G. J. Meyer, *Inorg. Chem.*, 1994, **33**, 5741–5749.
45 C.-Y. Chen, H.-C. Lu, C.-G. Wu, J.-G. Chen and K.-C. Ho, *Adv. Funct. Mater.*, 2007, **17**, 29–36.
46 K. A. Walters, L. Trouillet, S. Guillerez and K. S. Schanze, *Inorg. Chem.*, 2000, **39**, 5496–5509.
47 T. Pautzsch and E. Klemm, *Macromolecules*, 2002, **35**, 1569–1575.
48 M. J. Cook, A. P. Lewis, G. S. G. McAuliffe, V. Skarda, A. J. Thomson, J. L. Glasper and D. J. Robbins, *J. Chem. Soc., Perkin Trans. 2*, 1984, 1293–1301.
49 M. Maestri, N. Armaroli, V. Balzani, E. C. Constable and A. M. W. C. Thompson, *Inorg. Chem.*, 1995, **34**, 2759–2767.
50 R. Ziessel, V. Grosshenny, M. Hissler and C. Stroh, *Inorg. Chem.*, 2004, **43**, 4262–4271.
51 A. Barbieri, B. Ventura, F. Barigelletti, A. De Nicola, M. Quesada and R. Ziessel, *Inorg. Chem.*, 2004, **43**, 7359–7368.
52 A. Harriman, M. Hissler, A. Khatyr and R. Ziessel, *Eur. J. Inorg. Chem.*, 2003, 955–959.
53 A. Khatyr and R. Ziessel, *J. Org. Chem.*, 2000, **65**, 3126–3134.
54 S. S. Zhu, R. P. Kingsborough and T. M. Swager, *J. Mater. Chem.*, 1999, **9**, 2123–2131.
55 K. C. Zheng, J. P. Wang, W. L. Peng, X. W. Liu and F. C. Yun, *THEOCHEM*, 2002, **582**, 1–9.
56 H. Zabri, I. Gillaizeau, C. A. Bignozzi, S. Caramori, M.-F. Charlot, J. Cano-Boquera and F. Odobel, *Inorg. Chem.*, 2003, **42**, 6655–6666.
57 K. A. Walters, K. D. Ley, C. S. Cavalaheiro, S. E. Miller, D. Gosztola, M. R. Wasielewski, A. P. Bussandri, H. van Willigen and K. S. Schanze, *J. Am. Chem. Soc.*, 2001, **123**, 8329–8342.
58 K. A. Walters, K. D. Ley and K. S. Schanze, *Chem. Commun.*, 1998, 1115–1116.
59 A. Barbieri, B. Ventura, L. Flamigni, F. Barigelletti, G. Fuhrmann, P. Baeuerle, S. Goeb and R. Ziessel, *Inorg. Chem.*, 2005, **44**, 8033–8043.
60 O. Johansson, M. Borgström, R. Lomoth, M. Palmblad, J. Bergquist, L. Hammarström, L. Sun and B. Åkermark, *Inorg. Chem.*, 2003, **42**, 2908–2918.
61 J. Wiberg, L. Guo, K. Pettersson, D. Nilsson, T. Ljungdahl, J. Martensson and B. Albinsson, *J. Am. Chem. Soc.*, 2007, **129**, 155–163.
62 B. D. Allen, A. C. Benniston, A. Harrimann, L. J. Mallon and C. Pariani, *Phys. Chem. Chem. Phys.*, 2006, **8**, 4112–4118.
63 M. Borgström, O. Johansson, R. Lomoth, H. B. Baudin, S. Wallin, L. Sun, B. Akermark and L. Hammarstrom, *Inorg. Chem.*, 2003, **42**, 5173–5184.
64 C. H. Bamford and C. F. H. Tipper, *Comprehensive Chemical Kinetics; The Theory of Kinetics*, Amsterdam, 1969.
65 A. Yoshimura, M. Z. Hoffman and H. Sun, *J. Photochem. Photobiol., A*, 1993, **70**, 29–33.

